Mesenchymal Stem Cell-Derived Microvesicles Protect Against Acute Tubular Injury

Stefania Bruno,* Cristina Grange,* Maria Chiara Deregibus,* Raffaele A. Calogero,† Silvia Saviozzi,† Federica Collino,* Laura Morando,* Alessandro Busca,‡ Michele Falda,‡ Benedetta Bussolati,* Ciro Tetta,§ and Giovanni Camussi*

*Department of Internal Medicine, Research Center for Experimental Medicine and Center for Molecular Biotechnology, and †Department of Clinical and Biological Sciences, University of Torino, Torino, Italy; ‡Bone Marrow Transplant Unit, Haematological Division, San Giovanni Battista Hospital, Torino; §Fresenius Medical Care, Bad Homburg, Germany

ABSTRACT

Administration of mesenchymal stem cells (MSCs) improves the recovery from acute kidney injury (AKI). The mechanism may involve paracrine factors promoting proliferation of surviving intrinsic epithelial cells, but these factors remain unknown. In the current study, we found that microvesicles derived from human bone marrow MSCs stimulated proliferation *in vitro* and conferred resistance of tubular epithelial cells to apoptosis. The biologic action of microvesicles required their CD44- and β1-integrin-dependent incorporation into tubular cells. *In vivo*, microvesicles accelerated the morphologic and functional recovery of glycerol-induced AKI in SCID mice by inducing proliferation of tubular cells. The effect of microvesicles on the recovery of AKI was similar to the effect of human MSCs. RNase abolished the aforementioned effects of microvesicles *in vitro* and *in vivo*, suggesting RNA-dependent biologic effects. Microarray analysis and quantitative real time PCR of microvesicle-RNA extracts indicate that microvesicles shuttle a specific subset of cellular mRNA, such as mRNAs associated with the mesenchymal phenotype and with control of transcription, proliferation, and immunoregulation. These results suggest that microvesicles derived from MSCs may activate a proliferative program in surviving tubular cells after injury via a horizontal transfer of mRNA.

J Am Soc Nephrol 20: 1053–1067, 2009. doi: 10.1681/ASN.2008070798

Several studies demonstrate that the administration of exogenous mesenchymal stem cells (MSCs) contributes to the recovery of tissue injury in several organs such as heart, liver, brain, and pancreas.[1] Recently, the administration of *in vitro* expanded MSCs was shown to improve acute kidney injury (AKI).[2–8] Indeed, the infusion of MSCs protected and accelerated the recovery from AKI induced by *cis*-platinum,[3,4,9] glycerol,[5,6] and ischemia-reperfusion injury.[7,8] The mechanisms involved remain controversial. Some experiments based on bone marrow transplantation indicated that bone marrow-derived stem cells may contribute to repopulate the injured nephrons.[10,11] MSCs were shown to localize within the injured kidneys when injected in mice with AKI.[3,5,6,12] However, several reports indicate only a transient recruitment of MSCs in the renal vasculature without a direct incorporation within the regenerating tubules.[7,8,13] It was suggested that the transient presence of MSCs within the injured kidney may provide a paracrine support to the repair, which is mainly sustained by intrinsic epithelial cells surviving injury.[2,14] Recently Bi *et al.*[9]

Received July 29, 2008. Accepted December 30, 2008.

Published online ahead of print. Publication date available at www.jasn.org.

Correspondence: Dr. G. Camussi, Dipartimento di Medicina Interna, Ospedale Maggiore S. Giovanni Battista, Corso Dogliotti 14, 10126, Torino, Italy. Phone: +39-011-6336708; Fax: +39-011-6631184; E-mail: giovanni.camussi@unito.it

showed that MSCs may protect the kidney from toxic injury by producing factors that limit apoptosis and enhance proliferation of the endogenous tubular cells, suggesting that the tubular engraftment of MSCs is not necessary for their beneficial effect.

Besides soluble factors, cell-derived microvesicles (MVs) were described as a new mechanism of cell-to-cell communication.[15] MVs are released by various cell types[15,16] including stem cells and progenitors.[17,18] MVs may interact with target cells by surface-expressed ligands, transfer surface receptors, deliver proteins, mRNA, and bioactive lipids.[15] Ratajczak *et al.*[17] showed that MVs derived from embryonic stem cells may reprogram hematopoietic progenitors by an mRNA-dependent mechanism. Recently, we demonstrated that MVs derived from human endothelial progenitor cells (EPCs) are able to trigger angiogenesis in human vascular endothelial cells by a horizontal transfer of mRNA.[18]

In the present study, MVs obtained from human MSCs were characterized for the expression of surface molecules and for their mRNA content. Moreover, we evaluated whether administration of MSC-derived MVs in SCID mice with glycerol-induced AKI may favor functional and morphologic recovery. The effect of MVs was compared with that of MSC administration.

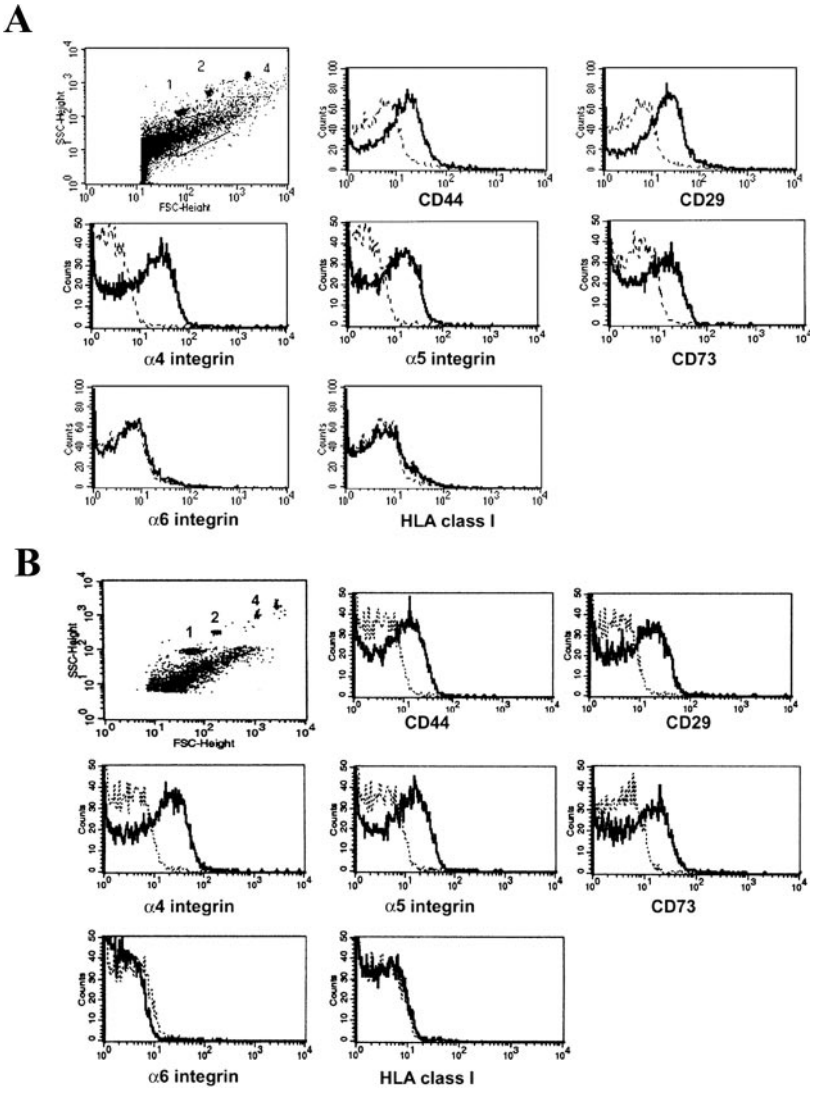

Figure 1. Cytofluorimetric characterization of mesenchymal stem cell (MSC)-derived microvesicles (MVs). Representative FACS analyses of MVs (A) and MVs treated with RNase (B) showing the size (with 1-, 2- and −4-μm beads used as internal size standards) and the expression of CD44, CD29, α-4 integrin, α-5 integrin, CD73, α-6 integrin, and HLA-class I (thick lines) surface molecules. Dot lines indicate the isotypic controls. Ten different MV preparations were analyzed with similar results. In the CD44, CD29, α-4 integrin, α-5 integrin, and CD73 experiments, the Kolmogrov-Smirnov statistical analyses between relevant antibodies and the isotypic control was significant ($P < 0.001$). No significant expression of α-5-integrin and HLA class I was observed.

RESULTS

Characterization of MSC-Derived MVs

By cytofluorimetric analyses, MVs were detected mainly below the forward scatter signal corresponding to 1-μm beads (Figure 1A). When determined by Zetasizer, the size of MVs ranged from 80 nm to 1 μm, with a mean value of 135 nm. Transmission and scanning electron microscopy performed on purified MVs showed their spheroid morphology and confirmed their size (Figure 2 A and B). When electron microscopy was performed on MSCs cultured overnight in serum-free condition, structures resembling MVs were found within larger vesicles in the cytoplasm or dismissed from the cell surface (Figure 2 C, D, and E). Cytofluorimetric analyses showed the presence of several adhesion molecules known to be expressed on MSC plasma membrane such as CD44, CD29, α4- and α5 integrins, and CD73, but not α6-integrin (Figure 1A). In addition, MVs did not express HLA-class I at variance with the cells of origin.

Gene Array Analyses of MSC-Derived MVs

MVs contained mRNA that was submitted to microarray analysis, not to define the amount of mRNA, but only to define which transcripts were present.[18,19] A total of 239 transcripts were found with this procedure; 132 were associated to Entrez Gene identifiers[20] by IPA 6.0 analysis (additional information: Table 1). This observation indicated that MVs shuttled a specific subset rather than a random sample of cellular mRNA. Several mRNA characteristic of mesenchymal cell lineages, such as neural, osteogenic, epithelial, and hematopoietic, were present (Table 1). Moreover, MVs contained mRNA related to several cell functions involved in the control of transcription, cell proliferation, and immune regulation (Table 2). Quantita-

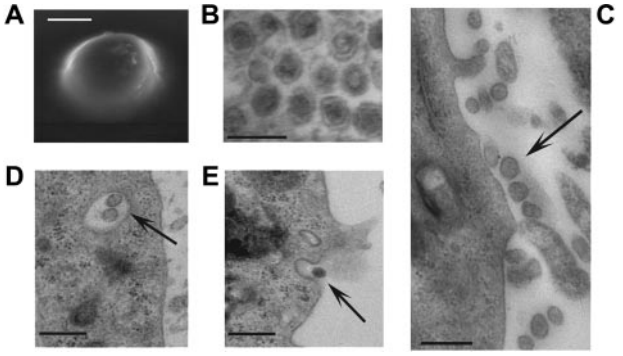

Figure 2. Electron microscopy analyses of microvesicles (MVs). (A) Representative micrographs of scanning electron microscopy of purified MSC-derived MVs showing a spheroid shape (white line = 100 nm). Images were obtained by secondary electron at a working distance of 15 to 25 mm and an accelerating voltage of 20 and 30 kV. Digital acquisition and analysis were performed using the Jeol T300 system. (B–E) Representative micrographs of transmission electron microscopy obtained on purified MVs (B) and on the MSC monolayer cultured over night in the medium used for collection of MVs (see Concise Methods). C shows the release of MVs from the surface of a MSCs; D shows the presence of MVs within larger vesicles in the cell cytoplasm. E shows the extrusion of a MV from the surface of a MSC. Ultrathin sections, stained with led citrate were viewed by JEOL Jem 1010 electron microscope (black line = 500 nm).

tive real time PCR confirmed the presence in MVs of genes randomly chosen from those detected by Microarray (*POLR2E*, *SENP2/SUMO1*, *RBL1*, *CXCR7*, *LTA4H*).

Incorporation of MSC-Derived MVs in Tubular Cells

MVs labeled with PKH26 dye were incorporated by cultured tubular epithelial cells (TECs) as shown by confocal microscopy and FACS analysis (Figure 3 A,B). MV treatment with soluble hyaluronic acid and anti-CD44 and -CD29 blocking antibodies inhibited MV incorporation in TECs, whereas anti-α4-integrin (Figure 3) and α5-integrin (not shown) did not prevent MV internalization, suggesting that expression of CD44 and CD29 is critical for their internalization. Moreover, removal of surface molecules by trypsin treatment of MVs inhibited their incorporation in TECs, confirming the relevance of surface molecules in MV internalization (Figure 3 A,B).

In Vitro Proliferative and Antiapoptotic Effects of MSC-Derived MVs

Incubation of TECs with different doses of MVs promoted cell proliferation compared with control cells incubated with vehicle alone (Figure 4A) and induced synthesis of hepatocyte growth factor (HGF) and macrophage-stimulating protein (MSP) (Figure 4B). In addition, incubation of TECs with MVs significantly inhibited apoptosis induced by serum deprivation (Figure 4C), vincristine, and *cis*-platinum (Figure 4D). MV treatment with soluble hyaluronic acid or trypsin, which inhibited MV incorporation, also inhibited the proliferative and antiapoptotic effects on TECs (Figure 4 A and B), suggesting that MV incorporation was required for their activity. However, when MVs were incubated with RNase that induced a complete degradation of the RNA shuttled by MVs,[18] the proliferation and the anti-apoptotic effects elicited by MVs were significantly reduced (Figure 4 A, C, and D). Figure 1B shows by FACS analyses that size and expression of surface adhesion molecules did not change in RNase-treated MVs. Moreover, internalization of RNase-treated MVs in TECs did not differ form that of untreated MVs (Figure 3B). DNase treatment was ineffective (not shown). RNase treatment of MVs did not interfere *per se* with TEC proliferation induced by the EGF (Figure 4A). These results suggest that the MV biologic effects were mediated by the transfer of mRNA following MV internalization as described previously for EPC-derived MVs.[18] MV derived from human fibroblasts did not stimulate TEC proliferation nor inhibited apoptosis (data not shown).

In Vitro Evidence of *De Novo* Human Protein Expression in Murine TECs by MV-Mediated Horizontal Transfer of mRNA

We used as reporter genes *POLR2E* and *SUMO-1*, which were present in MVs derived from human MSCs. Human *POLR2E* and *SUMO-1* were detected by real time PCR (RT-PCR) after 1 and 3 h of MV incubation with TECs (Figure 5A). The primers used did not recognize murine mRNA, as seen by negative RT-PCR in RNA extracted from control murine TECs. *De novo* cytoplasmic expression of human POLR2E protein and cytoplasmic and nuclear expression of SUMO-1 protein were detected in murine TECs after 24 h incubation with MVs (Figure 5 B). Nuclear localization of both proteins was observed after 48 h (Figure 5B).

MSC-Derived MVs Protect Against Glycerol-Induced AKI

We compared the effect of human MSCs and MSC-derived MVs injected intravenously in glycerol-induced AKI in SCID mice (Figure 6). Three days after glycerol injection, we observed a significant rise in blood urea nitrogen (BUN) and creatinine (Figure 7A) associated with a marked tubular epithelial injury, whereas control mice injected with saline alone displayed no histologic alterations (not shown). At day 3, MSCs or MSC-derived MVs were injected intravenously at doses of 75,000 cells (an amount of cells releasing approximately 15 μg MVs overnight) or 15 μg MV proteins, respectively . Mice were sacrificed at 4, 5, 8, and 15 d after induction of AKI (Figure 6). The lesions observed in mice with AKI at days 4, 5, and 8 included tubular hyaline casts, vacuolization, and widespread necrosis of proximal and distal tubular epithelium (Figure 7B). Proximal tubules showed cytoplasmic vacuolization, swelling and disorganization of mitochondria, loss of brush border, and denudation of basal membrane (Figure 8 B and C). When mice were treated with MSCs or MVs, the tubular lesions were less severe at day 5 and almost absent at day 8 compared to those of mice treated with vehicle alone

Table 1. MV-shuttled mRNA involved in cell differentiation

Differentiation	Gene Name	Description
Neural	*RAX2*	Retina and anterior neural fold homeobox 2
	OR11H12	Olfactory receptor, family 11, subfamily H, member 12
	OR2M3	Olfactory receptor, family 2, subfamily M, member 3
	DDN	Dendrin
	GRIN3A	Glutamate receptor, 3A
Bone	*NIN*	Ninein (GSK3B interacting protein)
	BMP15	Bone morphogenetic protein 15
	IBSP	Bone sialoprotein II
Endo/epithelial	*MAGED2*	Melanoma antigen family D, 2
	CEACAM5	Carcinoembryonic antigen-related cell adhesion molecule
	COL4A2	Collagen, type IV, alpha 2
	SCNN1G	Sodium channel, nonvoltage-gated1, gamma
	PKD2L2	Polycystic kidney disease 2-like 2
Hematopoietic	*HK3*	Hexokinase 3 (white cell)
	EPX	Eosinophil peroxidase

Table 2. MV-shuttled mRNA involved in transcription, cell proliferation, and immune regulation

Functional Category	mRNA	Description
Transcription factors	CLOCK	Clock homolog (mouse)
	IRF6	Interferon regulatory factor 6
	LHX6	LIM homeobox 6
	RAX2	Retina and anterior neural fold homeobox 2
	TCFP2	Transcription factor CP2
	BCL6B	B-cell CLL/lymphoma 6, member B
DNA/RNA binding	HMGN4	High mobility group nucleosomal binding domain 4
	TOPORS	Topoisomerase I binding, arginine/serine rich
	ESF1	Nuclear pre-rRNA processing protein
	POLR2E	Polymerase (RNA) II (DNA-directed) polypeptide E, 25 kDa
	ELP4	Elongation protein 4 homolog
	HNRPH2	Heterogeneous nuclear ribonucleoprotein H2
Cell Cycle	SENP2	SUMO1
	RBL1	Retinoblastoma-like 1 (p107)
	CDC14B	CDC14 cells division cycle 14 homolog B
	S100A13	S100 calcium binding protein A13
Receptors	CEACAM5	Carcinoembryonic antigen-related cell adhesion molecule 5
	CLEC2A	C-type lectin domain family 2, member A
	CXCR7	Chemokine (C-X-C motif) receptor 7
Enzymes/metabolism	ADAM15	ADAM metallopeptidase domain 15
	FUT3	Fucosyltransferase 3
	ADM2	Adrenomedullin 2
	LTA4H	Leukotriene A4 hydrolase
	BDH2	3-Hydroxybutyrate dehydrogenase, type 2
	RAB5A	RAB5A, member RAS oncogene family
Immune regulation	CRLF1	Cytokine receptor-like factor 1
	IL1RN	Interleukin 1 receptor antagonist
	MT1X	Metallothionein 1X
Cytoskeleton	DDN	Dendrin
	MSN	Moesin
	CTNNA1	Catenin (cadherin-associated protein)
Extracellular matrix	COL4A2	Collagen type IV, alpha 2
	IBSP	Bone sialoprotein II

(Figure 7B). The quantitative evaluation of casts and tubular necrosis at day 5 showed a significant reduction in MV- and MSC-treated mice in parallel with the reduction of BUN (Table 3). The recovery was complete at day 15 (not shown). By electron microscopy, tubular cells in MV-treated AKI mice showed a marked increase of mitochondria at day 5 that was decreased at day 8. In addition, the brush border was already restored at day 5, and the ultrastructure of tubules was almost

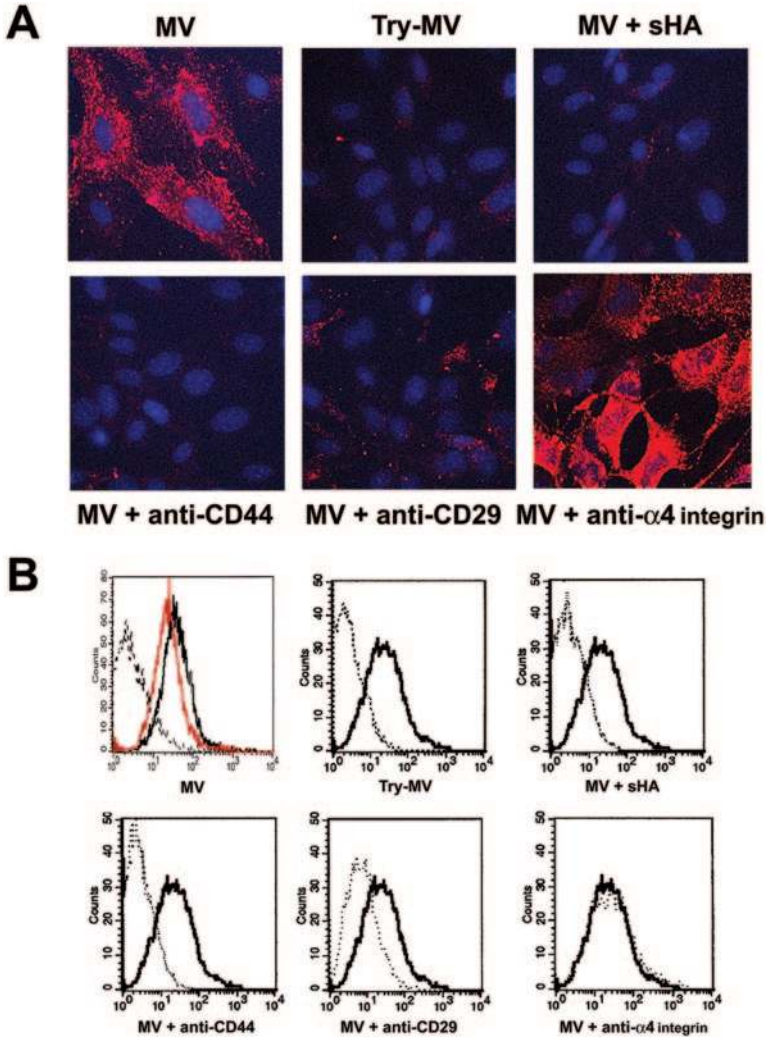

Figure 3. Incorporation of MVs in tubular epithelial cells (TECs). (A) Representative micrographs of internalization by TECs (30 min at 37 °C) of microvesicles (MVs) labeled with PKH26 preincubated or not with trypsin (0.5 mM) (Try); or with 100 μg/ml of sHA; or with 1 μg/ml blocking monoclonal antibody against CD44, CD29, and α4 integrin. Three experiments were performed with similar results. (B) Representative FACS analyses of internalization, after 30 min of incubation at 37 °C, by TECs of MVs labeled with PKH26 (black curves) preincubated or not with trypsin (Try) or with 100 μg/ml of sHA or with 1 μg/ml blocking monoclonal antibodies against CD44, CD29, and α4 integrin. Black curves indicate the internalization of untreated MVs. In the first panel, dot curve indicates the negative control (cells not incubated with MVs); red curve indicates the MVs treated with RNase and labeled with PKH26. In the other panels, dot curves indicate internalization of MVs after pretreatment with trypsin or incubation with blocking antibodies or sHA. Three experiments were performed with similar results.

indistinguishable from that of control mice without AKI (Figure 8). In addition, MSC- and MV- treated mice showed a significant reduction of both BUN and creatinine (Figure 7A). There was no significant difference between the treatment with MSCs and that of MVs (Figure 7, Table 3). In addition, MVs treated with sHA or trypsin did not significantly improve functional and morphologic injury compared with untreated AKI (Table 3). The specificity of MSC-derived MVs was also indicated by the absence of protective effects of MVs derived from human fibroblasts (Table 3).

As shown in Figure 9, MV treatment of mice with AKI significantly enhanced tubular cell proliferation compared to treatment with vehicle alone, as detected by PCNA- and 5-bromo-2′-deoxy-uridine (BrdU)-positive cells. The enhanced proliferation was detected 24 h (day 4 of AKI) and 48 h (day 5 of AKI) after MV administration and found to decrease thereafter. MSC treatment induced a comparable enhancement of cell proliferation (Figure 9). The majority of PCNA- and BrdU-positive cells, seen in MV- and in MSC- injected animals, were located in distal and proximal tubules. On the contrary, in untreated mice with AKI, proliferation was delayed as the number of PCNA- and BrdU positive cells increased only at day 8 when no further proliferation was detected in mice with AKI treated with MVs or MSCs. sHA-treated MVs as well as fibroblast-derived MVs did not significantly enhance proliferation (Figure 9 A and B).

Evaluation of MV Localization After *In Vivo* Injection

When labeled MVs were injected, a significant accumulation in the kidney was observed at 6 h only in AKI mice (Figure 10A). After 1 h, MVs were detectable within the endothelial cells of large vessels and within the lumen of some injured tubules (Figure 10B). After 3 h, several tubular cells contained labeled MVs (Figure 10 C and D). The amount of tubular cells containing MVs was markedly enhanced at 6 h (Figure 10 E and F). When injected in normal control mice, the accumulation was significantly lower than in AKI, and MVs were not detected in tubular cells (Figure 10 A and H). In plasma, the concentration of MVs significantly decreased in AKI but not in normal controls (Figure 10A). Trypsin-treated MVs were not detected in the kidney of AKI mice and remained constant in plasma at any time (Figure 10 A,G). MVs were minimally detected in the lung (Figure 10A) and as shown by confocal microscopy were mainly located in the endothelial cells of large vessels and not in the alveolar capillaries (Figure 10 J and K). In contrast, liver accumulation of MVs was detected both in normal controls and in AKI mice (Figure 10 A and L). Trypsin-treated MVs did not localize in any of the examined organs (Figure 10A).

RNA Shuttled by MV Mediates MV-Induced Recovery of AKI

As shown in Figure 7 and in Table 3, RNase treatment significantly reduced the recovery of BUN, creatinine, and tubular lesions that did not differ from those of untreated mice with AKI. Moreover at

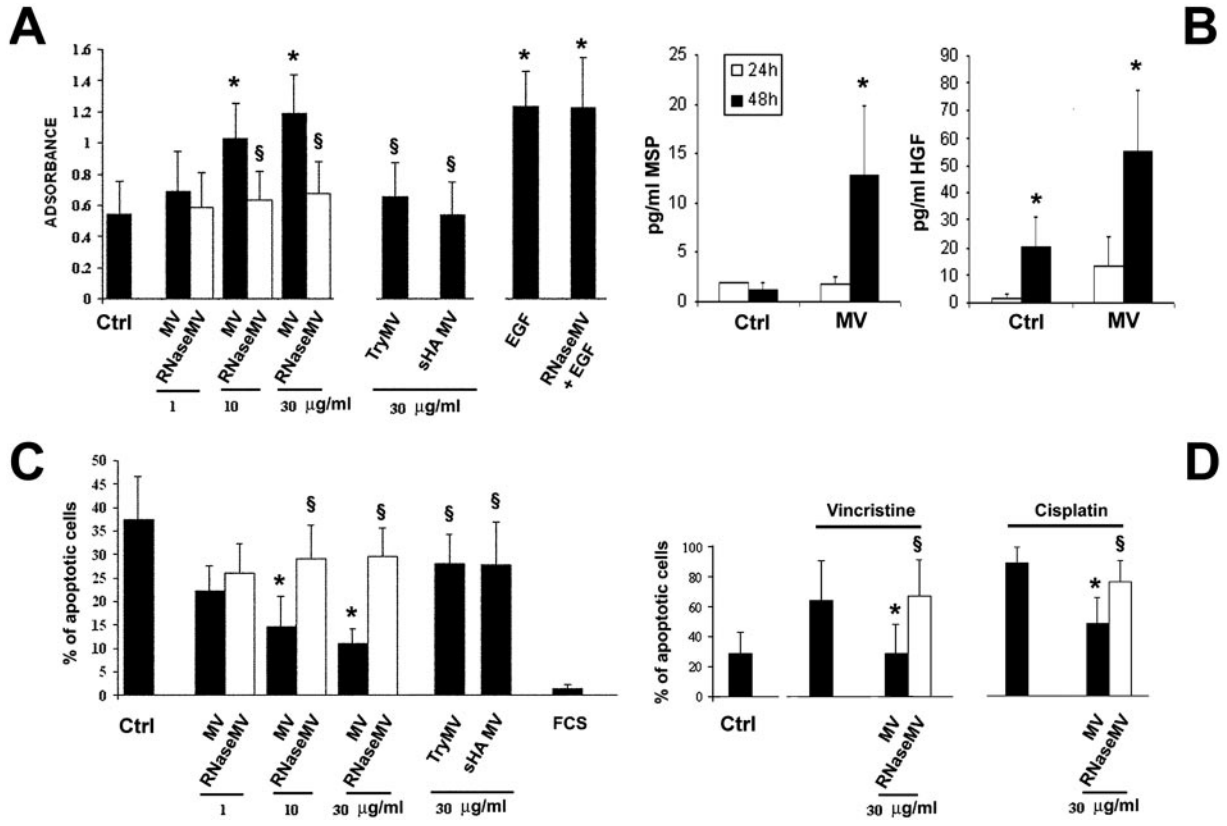

Figure 4. Proliferative and anti-apoptotic effects of mesenchymal stem cell (MSC)-derived microvesicles (MVs). (A) 10 μM BrdU was added to 4000 cells/well (TECs) into 96-well plates incubated for 48 h in DMEM deprived of FCS in the presence of vehicle alone or of different doses of MVs (black bars) or of RNase-treated MVs (white bars) or MVs pretreated with trypsin or with 100 μg/ml of sHA. EGF-induced (10 ng/ml) proliferation was also evaluated in TECs incubated or not with RNase-pretreated MVs (30 μg/ml). Results are expressed as mean ± SD of six different experiments. ANOVA with Newmann-Keuls multicomparison test was performed; *$P < 0.05$ MVs or EGF *versus* vehicle alone; §$P < 0.05$ MVs untreated *versus* MV treated with RNase, trypsin (Try-MV) or sHA. (B) Release of MSP and HGF by 1×10^5 TECs incubated for 24 or 48 h with 30 μg/ml MVs compared with TECs incubated with vehicle alone (Ctrl). Results are expressed mean ± SD of six experiments, and *t* test was performed between MV treatment and control; *$P < 0.05$. (C) The percentage of apoptotic cells after 48-h serum deprivation (0% FCS, Ctrl) was evaluated by the TUNEL assay. TECs were incubated with vehicle alone, or with different doses of MVs (black bars) or of RNase-treated MVs (white bars), or MVs pretreated with trypsin or with 100 μg/ml of sHA. Results are expressed as mean ± SD of six different experiments. ANOVA of variance with Newmann-Keuls multicomparison test was performed; *$P < 0.05$ MVs *versus* vehicle alone; §$P < 0.05$ MVs treated *versus* MVs untreated. (D) The percentage of apoptotic cells after 48-h incubation with 100 ng/ml of vincristine or 5 μg/ml of cisplatinum was evaluated by the TUNEL assay. TECs were incubated with the apoptotic stimuli with or without 30 μg/ml MVs (black bars) or RNase-treated MVs (white bars) in the presence of 3% FCS (Ctrl = TECs incubated 48 h in the presence of 3% FCS only). Results are expressed as mean ± SD of six different experiments. Analyses of variance with Newmann-Keuls multicomparison test was performed; $P < 0.05$ MVs *versus* vehicle alone; §$P < 0.05$ MVs treated *versus* MV untreated.

day 8, in mice injected with MVs treated with RNase, the lesions persisted, with an increase in tubular casts and aspect of epithelial atrophy (Figure 7B). Tubular cell proliferation detected as BrdU- or PCNA-positive cells in mice injected with RNase-treated MVs did not differ from that of untreated mice with AKI (Figure 9).

In Vivo Evidence of *De Novo* Human Proteins Expression in the Kidney of AKI Mice Treated with Human MVs

RT-PCR for human *POLR2E*, used as reporter gene, confirmed the accumulation of MVs within the kidney of MV-treated AKI mice and not in normal controls (Figure 11A). Using anti-human POLR2E and SUMO-1 antibodies, the proteins were detected with a nuclear localization in tubules of mice with AKI treated with MV but not in untreated mice (Figure 11B). This observation suggests that specific mRNA shuttled by MVs can also be translated *in vivo* in proteins.

DISCUSSION

In the present study, we demonstrated that MVs derived from human MSCs are able to stimulate *in vitro* proliferation and apoptosis resistance of TECs and to accelerate *in vivo* the recovery of glycerol-induced AKI in SCID mice. The effect of

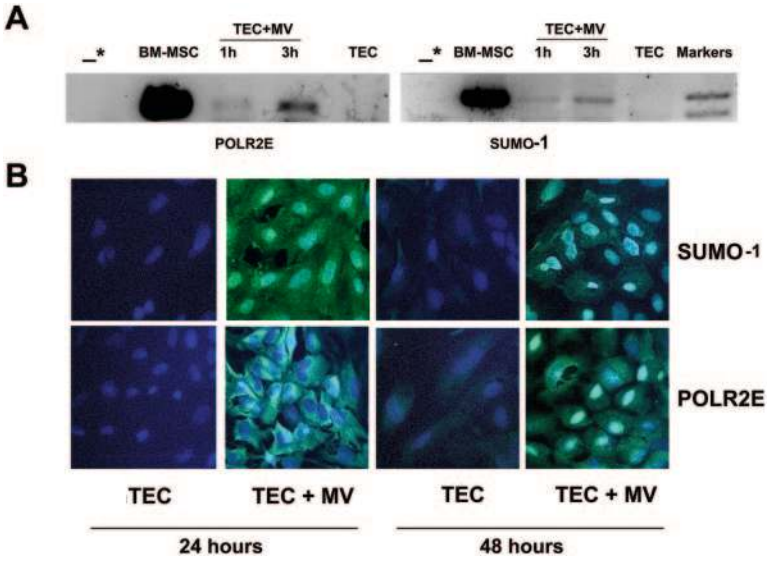

Figure 5. mRNA horizontal transfer and human protein expression in tubular epithelial cells (TECs) treated with mesenchymal stem cell (MSC)-derived microvesicles (MVs). (A) 1×10^5 TECs cultured in the absence (TEC) or in the presence (TEC+MV) of 30 μg MVs for 1 and 3 h were analyzed by RT-PCR for specific human mRNA. Bands of PCR products specific for human POLR2E and SUMO-1 of the expected size (90 bp) were detected in a 4% agarose gel electrophoresis. As positive control the extract of human bone marrow-derived MSCs (BM-MSC) was used. The asterisk indicates the control without cDNA. B: Representative micrographs showing the expression of human POLR2E and SUMO-1 proteins by TECs, cultured in the absence or in the presence of 30 μg MVs for 24 and 48 h. After 24 h, POLR2E protein was detected in the cytoplasm and SUMO-1 in the cytoplasm and nuclei of TECs. After 48 h, both proteins were translocated to the nucleus. Nuclei were counterstained with Hoechst dye. Independent experiments using four different MV preparations were performed with similar results. Original magnification: ×630.

administration of MVs was comparable to that of human bone marrow-derived MSCs. The RNase treatment of MVs abrogated both the *in vitro* and *in vivo* effects of MVs, suggesting that the mRNA shuttled by MVs is the final effector of their biologic effects.

Several studies demonstrated that the administration of bone marrow-derived MSCs may protect and reverse AKI in different experimental models.[2–9] The low number of MSCs detectable within tubules after injury together with the increase in proliferating tubular cells throughout the kidney implies a trophic effect of MSCs on resident tubular cells that have survived injury, rather than a direct repopulation.[7,8,14] It was suggested that MSCs may exert their effects by a paracrine action on resident cells.[2,7,13,21,22] Recently, soluble factors were implicated in the MSC protective effect.[23] Bi *et al.*[9] showed that MSCs may protect the kidney from toxic injury by producing factors that limit apoptosis and enhance proliferation of the endogenous tubular cells, indicating that tubular engraftment of the MSCs is not necessary for their beneficial effect.

We demonstrated that intravenous administration of MVs derived from human MSCs has the same efficacy of MSCs on the functional and morphologic recovery of glycerol induced AKI in SCID mice. MVs are small vesicles released by cells that express the characteristic antigens of the cell from which they originate and carry membrane and cytoplasmic constituents.[15,16] MVs may interact with target cells through specific receptor–ligand interactions and transfer receptors, proteins, and bioactive lipids.[16] Moreover, several studies showed that MVs may shuttle selected patterns of mRNA and proposed this as a new mechanism of genetic exchange between cells.[17–19,24]

In the present study, we demonstrate that MVs derived from MSCs may induce *in vitro* proliferation and apoptosis resistance in TECs. It was previously reported that MVs may express surface molecules characteristic of originating cells.[16–18,25–27] We found that MSC-derived MVs expressed several adhesion molecules of MSCs such as CD44, CD29 (β1-integrin), α4- and α5 integrins, and CD73, but not α6 integrin. Some of these molecules, namely CD44 and CD29, were found to be instrumental in MV internalization into TECs, as treatment with sHA or with anti-CD44 and anti-CD29 blocking antibodies prevented MV incorporation. Moreover, we found that the internalization of MVs was a requirement, but not the mechanism responsible, for their biologic activity. Indeed, RNase treatment almost completely abrogated the MV-induced *in vitro* proliferation and resistance to apoptosis of TECs.

The *in vivo* administration of MVs was found to accelerate the functional and morphologic recovery of AKI. These biologic

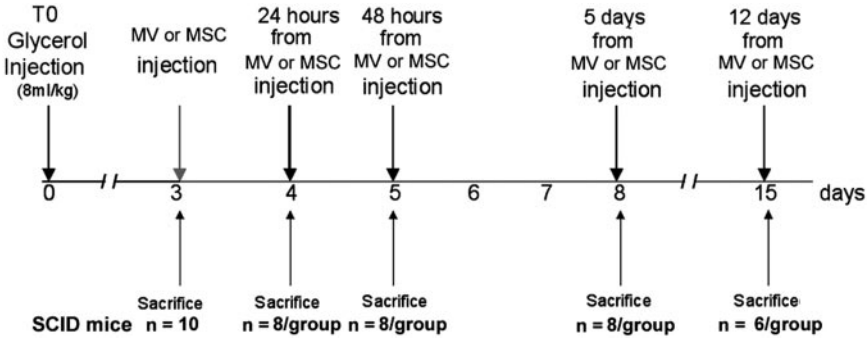

Figure 6. Schematic representation of the protocol of glycerol induced acute kidney injury (AKI) and treatment with mesenchymal stem cells (MSCs) or MSC-derived microvesicles (MVs). Glycerol was injected intramuscularly at time 0; the arrow at day 3 indicate the administration of 75,000 MSCs; or 15 μg of MSC-derived MVs; or MSC-derived MVs treated with RNase, trypsin, or sHA; or fibroblast-derived MVs; or vehicle alone; the subsequent arrows indicate the time of sacrifice.

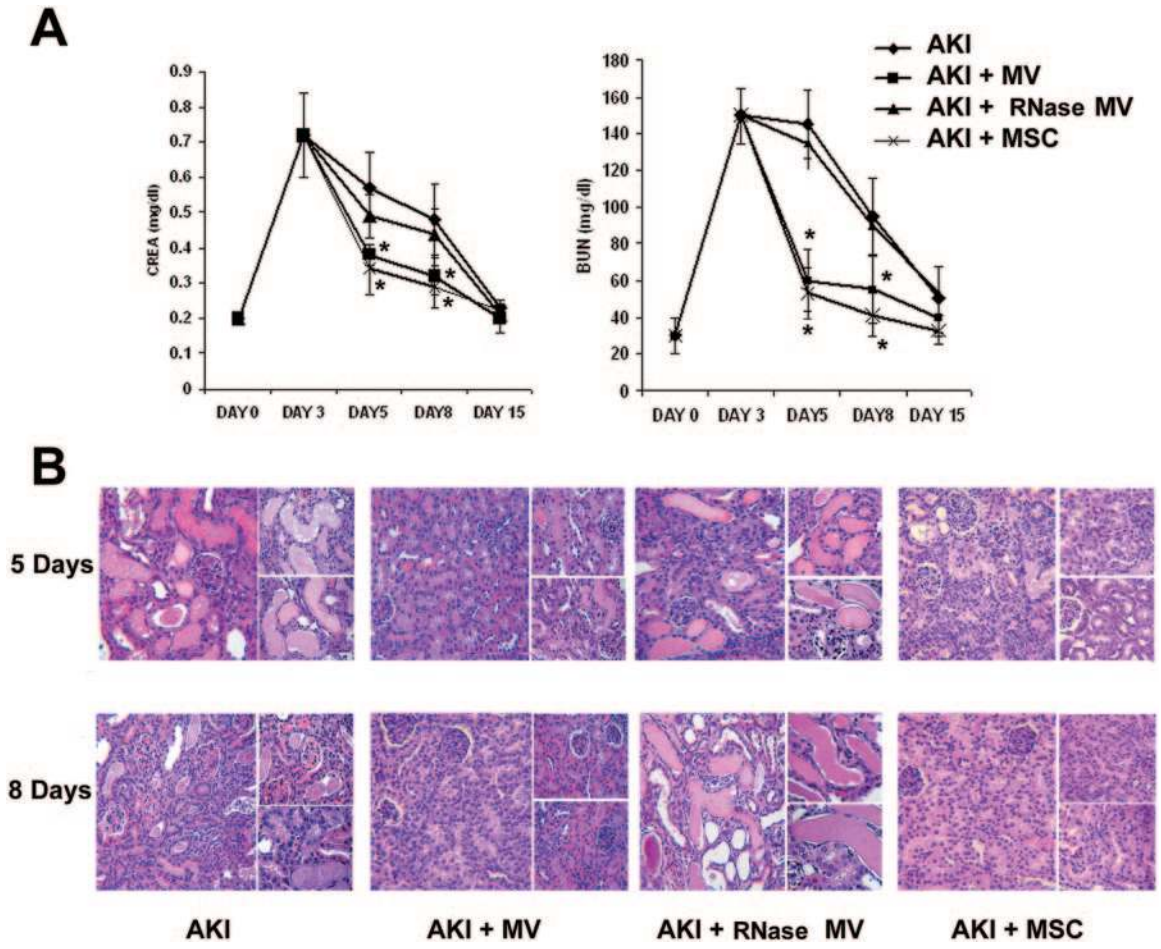

Figure 7. Effects of intravenous injection of microvesicles (MVs) or mesenchymal stem cells (MSCs) into acute kidney injury (AKI) mice. Mice were given intramuscular injection of 8 ml/kg of 50% glycerol on day 0, followed by intravenous injection of MVs or RNase-treated MVs or MSCs or vehicle as control on day 3. (A and B) Creatinine and blood urea nitrogen values at the beginning of the experiments and on day 3, 5, 8, and 15 after glycerol administration. ANOVA with Dunnet's multicomparison test: $*P < 0.05$ MV- or MSC- treated AKI mice *versus* control AKI mice. (C) Representative micrographs of renal histology at day 5 and 8 after glycerol administration in control AKI mice, in AKI mice injected with 15 μg of MVs or RNase-MV or with 75,000 MSCs. Magnification: ×400.

effects were specific for MSC-derived MVs as MVs obtained form fibroblasts were ineffective, and involved MV adhesion molecules as trypsin treatment abrogated MV accumulation in the kidney. MVs accumulated within the lumen of injured tubules, thus allowing an uptake from the apical part of tubular cells that survived injury. In addition, an uptake by endothelial cells was observed, suggesting that MVs may also reach the basolateral side of tubular cells *via* peritubular capillaries. Apart from inducing TEC proliferation, MVs may act by a mechanism of renal protection that limits the extent of injury. However, in the present experimental setting, MVs were administered at the peak of functional and morphologic alterations.[5,6]

As seen *in vitro*, pretreatment of MVs with RNase abrogated the protective effect of MVs. These results suggest that the transfer of small amounts of exogenous mRNA may stimulate tubular cell regeneration. Indeed, MVs derived from MSCs contained mRNA associated with the mesenchymal differentiative phenotype and with several cell functions involved in the control of transcription, proliferation, and cell immune regulation. Interestingly, as in EPC-derived MVs, MVs from MSCs carried a gene encoding the polymerase responsible for synthesizing mRNA in eukaryotes.[28] *In vitro* evidence for an effective horizontal transfer of mRNA was obtained by the presence of the human-specific mRNA for *POLR2E* and *SUMO-1* and by their *de novo* protein expression in MV-treated TECs. *In vivo* expression of human POLR2E and SUMO-1 proteins in tubular cells was also detected in mice with AKI treated with MVs. MV-mediated transfer of mRNA/proteins derived from stem cells may therefore induce de-differentiation of mature cells, triggering a proliferative program that may contribute to the repair of tissue injury. Moreover, stimulation of TECs with MVs induced synthesis of HGF and MSP, although their mRNA was not included in MVs, suggesting that the activation of cellular pathways that generate a cascade of multiple mediators that may be concurrent with recovery from acute tubular injury.[29–31]

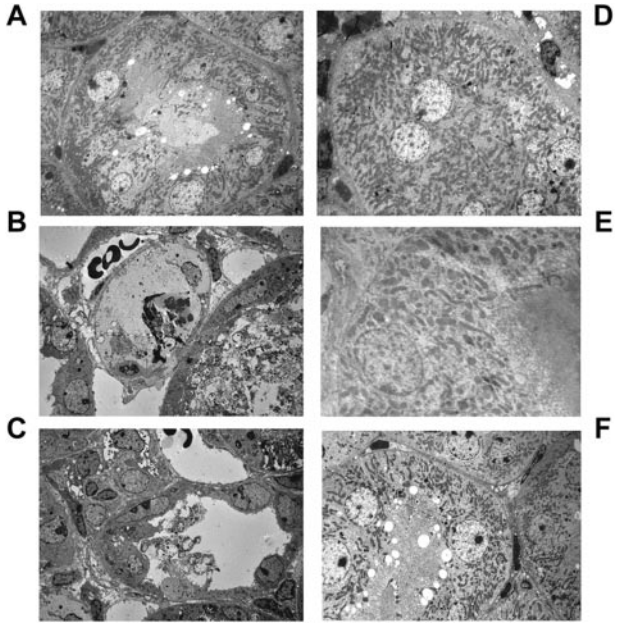

Figure 8. Ultrastructural changes of tubules in acute kidney injury (AKI) mice and effects of microvesicle (MV) injection. Representative electron micrographs of tubules of (A) normal control mouse, (B) AKI mouse at day 5 receiving saline, (C) AKI mouse at day 8 receiving saline, (D, E) MV-treated AKI mouse at day 5, and (F) MV-treated AKI mouse at day 8. Original magnification: A, D, F: ×3000; B, C: 2500; E: ×6000.

These studies open new research perspectives on the use of MVs to transfer RNA-based information from stem cells/precursors to target differentiated cells. An advantage of using MVs in regenerative medicine rather than the stem cells themselves is the avoidance of possible long-term pathologic differentiation of engrafted cells.[32]

In conclusion, the mRNA transfer from MSCs to target cells through internalization of MVs contribute along with soluble factors to the regenerative effect of MSCs and could be exploited as a new therapeutic approach for regenerative medicine.

CONCISE METHODS

Isolation and Characterization of Human MSCs

Approval of the study was obtained from the Center for Molecular Biotechnology Institutional Review Board. Bone marrow cells were harvested from 13 different healthy donors with informed consent obtained in accordance with the Declaration of Helsinki, or obtained by Lonza (Basel, Switzerland). Bone marrow cells were layered on a Ficoll gradient (density: 1022 g/ml; Sigma-Aldrich, St. Louis, MO) and centrifuged at 1500 rpm for 30 min. The mononucleated cells were cultured in the presence of mesenchymal stem cells basal medium (MSCBM, Lonza). After 5 d of culture, the medium was changed. To expand the isolated cells, the adherent monolayer was detached by trypsin treatment for 5 min at 37 °C, after 15 d for the first passage and every 7 d for successive passages. Cells were seeded at a density of 10,000 cells/cm^2 and used within the sixth passage.

At each passage, cells were counted and analyzed for immunophenotype by cytofluorimetric analysis and immunofluorescence. Cytofluorimetric analysis was performed as described[33] and the following antibodies, all phycoerythrin (PE) or FITC conjugated, were used: anti-CD105, -CD29, -CD31, -CD146, -CD44, -CD90 (Dako Cytomation, Copenhagen, Denmark); -CD73, -CD34, -CD45, -CD80, -CD86,-CD166, HLA-I (Becton Dickinson Biosciences Pharmingen, San Jose, CA); -CD133 (Miltenyi Biotec, Auburn); KDR (R&D Systems, Abington, U.K.); -HLA-II (Chemicon International Temecula, CA), -CD40 (Immunotech, Beckman Coulter), -CD154 (Serotec, Raleigh, NC) monoclonal antibodies. Mouse IgG isotypic controls were from Dako Cytomation.

Indirect immunofluorescence was performed on MSCs using the following antibodies: mouse monoclonal anti-vimentin (Sigma) and rabbit polyclonal anti-von Willebrand factor (Dako Cytomation). Omission of the primary antibodies or substitution with nonimmune rabbit or mouse IgG were used as controls where appropriated. Alexa Fluor 488 anti-rabbit and anti-mouse Texas Red (Molecular Probes, Leiden, the Netherlands) were used as secondary antibodies.

MSCs preparations did not express hematopoietic markers like CD45, CD14, and CD34. They also did not express the costimulatory molecules (CD80, CD86, and CD40) and the endothelial markers (CD31, von Willebrand factor, KDR). All of the cell preparations at different passages of culture expressed the typical MSC markers: CD105, CD73, CD44, CD90, CD166, and CD146. They also expressed HLA class I. The adipogenic, osteogenic, and chondrogenic differentiation ability of MSC was determined as described previously.[34]

Human fibroblasts, isolated from dermas as described[35] and used as control, were maintained in DMEM (Sigma) with 10% FCS (Euroclone, Wetherby, UK).

Table 3. Effect of MSCs, MSC-derived MVs, and fibroblast-derived MVs on renal morphology and function at day 5 after AKI induction

	Control	AKI	AKI + MV	AKI + MV RNasi	AKI + MSC	AKI + F-MV	AKI + MV sHA	AKI + Try-MV
Cast (n/HPF)	0	3.93 ± 1.02	0.45 ± 0.4[a]	2.86 ± 0.88	0.35 ± 0.31[a]	3.03 ± 0.32	2.38 ± 0.44	4.2 ± 2.36
Tubular necrosis (n/HPF)	0	3.27 ± 0.34	0.24 ± 0.06[a]	3.32 ± 1.5	0.38 ± 0.12[a]	3.49 ± 0.42	2.72 ± 0.64	3.78 ± 1.25
BUN (mg/dl)	30 ± 10	145 ± 20	60 ± 12[a]	135 ± 17	52.8 ± 14[a]	139 ± 18	133 ± 14	132 ± 19

Injection of 75,000 MSCs, of 15 μg of MSC-derived MVs with or without treatment with sHA or trypsin and 15 mg of fibroblast-derived MVs. Results are expressed as mean ± SD; ANOVA with Dunnet's multicomparison test: [a]$P < 0.05$ treatments vs untreated AKI. AKI; AKI untreated with MVs; AKI + MV; AKI treated MSC-derived MVs; AKI + RNase MV; AKI treated with RNase inactivated MSC-derived MVs; AKI + MSC; AKI treated with MSCs; AKI + MV sHA; AKI treated with MSC-derived MVs preincubated with sHA; AKI + F-MV; AKI treated with fibroblast-derived MVs.

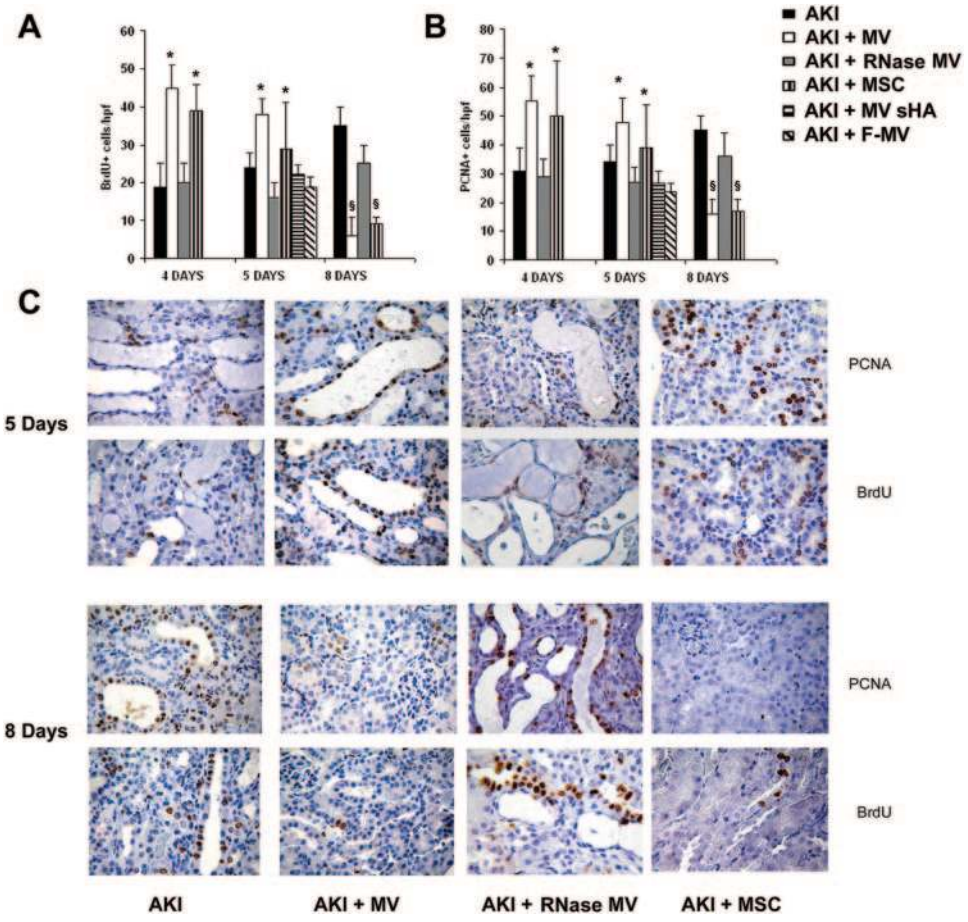

Figure 9. Renal cell proliferation in acute kidney injury (AKI) mice untreated or treated with MSCs or MVs. (A) Quantification of BrdU-positive cells/high power field (hpf). BrdU was injected intraperitoneally for 2 successive days before mice being killed. (B) Quantification of PCNA-positive cells/hpf. All quantitative data were obtained from eight different mice for experimental conditions. ANOVA with Dunnet's multicomparison test: $*P < 0.05$ MSC- or MV-injected mice *versus* AKI control mice. (C) Representative micrographs of PCNA or BrdU uptake staining performed on sections of kidneys 5 and 8 d after glycerol treatment (2 and 5 d after vehicle or MSC or MV injection). Magnification: ×400. AKI, AKI untreated with MVs; AKI+MV, AKI treated with 15 μg MSC-derived MVs; AKI+RNase MV, AKI treated with 15 μg RNase inactivated MSC-derived MVs; AKI+MSC, AKI treated with 75,000 MSCs; AKI+MV sHA, AKI treated with 15 μg MSC-derived MVs preincubated with sHA; AKI+F-MV, AKI treated with 15 μg fibroblast-derived MVs.

Isolation of MVs

MVs were obtained from supernatants of MSCs and of fibroblasts cultured in RPMI deprived of FCS and supplemented with 0.5% of BSA (Sigma). The viability of cells incubated overnight without serum was > 99% for MSCs and 85% ± 4.3% for fibroblast as detected by trypan blue exclusion. No apoptotic cells were detected by TUNEL assay in MSCs, and 3.2% ± 1.3% apoptotic cell were detected for fibroblast. After centrifugation at 2000 g for 20 min to remove debris, cell-free supernatants were centrifuged at 100,000 g (Beckman Coulter Optima L-90K ultracentrifuge) for 1 h at 4 °C, washed in serum-free medium 199 containing N-2-hydroxyethylpiperazine-N′-2-ethanesulfonic acid (HEPES) 25mM (Sigma) and submitted to a second ultracentrifugation in the same conditions.[17,18] To trace, *in vitro* and *in vivo*, MVs by fluorescence microscopy or FACS analysis, MVs from MSCs were labeled with the red fluorescence aliphatic chromophore intercalating into lipid bilayers PKH26 dye (Sigma).[36] After labeling, MVs were washed and ultracentrifuged at 100,000 g for 1 h at 4 °C. MV pellets were suspended in medium 199, and the protein content was quantified by the Bradford method (BioRad, Hercules, CA). Endotoxin contamination of MVs was excluded by Limulus testing according to the manufacturer's instruction (Charles River Laboratories, Inc., Wilmington, MA), and MV were stored at −80 °C. The morphologic analyses performed on MV suspension after staining with propidium iodide did not show the presence of apoptotic bodies.

In selected experiments, MVs from MSCs were treated with 1 U/ml RNase (Ambion Inc., Austin, TX) for 1 h at 37 °C, the reaction was stopped by addition of 10 U/ml RNase inhibitor (Ambion Inc.) and MVs were washed by ultracentrifugation.[17,18] The effectiveness of RNase treatment was evaluated after RNA extraction using TRIZOL reagent (Invitrogen, Carlsbad, CA) by spectrophotometer analysis of total extracted RNA (untreated: 1.3 ± 0.2 μg RNA/ mg protein MV; RNase treated: <0.2 μg RNA/mg protein MV). In addition, RNA extracted from RNase-treated and untreated MVs was labeled by oligo dT driven retrotranscription and analyzed on 0.6% agarose gel to show the complete degradation of RNA by RNase treatment, as described previously.[18] As control, MVs were treated with 1 U/ml DNase (Ambion Inc.) for 1 h at 37 °C.

FACS Analysis of MVs

The size of MVs was determined by cytofluorimetic analyses. The instrument was rinsed with particle-free rinse solution for 15 min to eliminate the background. The beads of different sizes (1, 2, 4, and 6 μm, Molecular Probes, Invitrogen) were used as the size markers, and analysis was performed using a log scale for forward scatter and side scatter parameters. Moreover, the size of MV was evaluated by the Zetasizer Nano (Malvern Instruments, Malvern Worcestershire, UK) instrument, which permits discrimination of microparticles less than 1 μm in diameter. Cytofluorimetric analysis was performed as described previously,[18,37] using the following FITC- or PE-conjugated antibodies: CD146, CD44 (Dako Cytomation), CD133 (Miltenyi Biotec), CD73, ICAM-1, α4-integrin, (Becton Dickinson), αvβ3-inte-

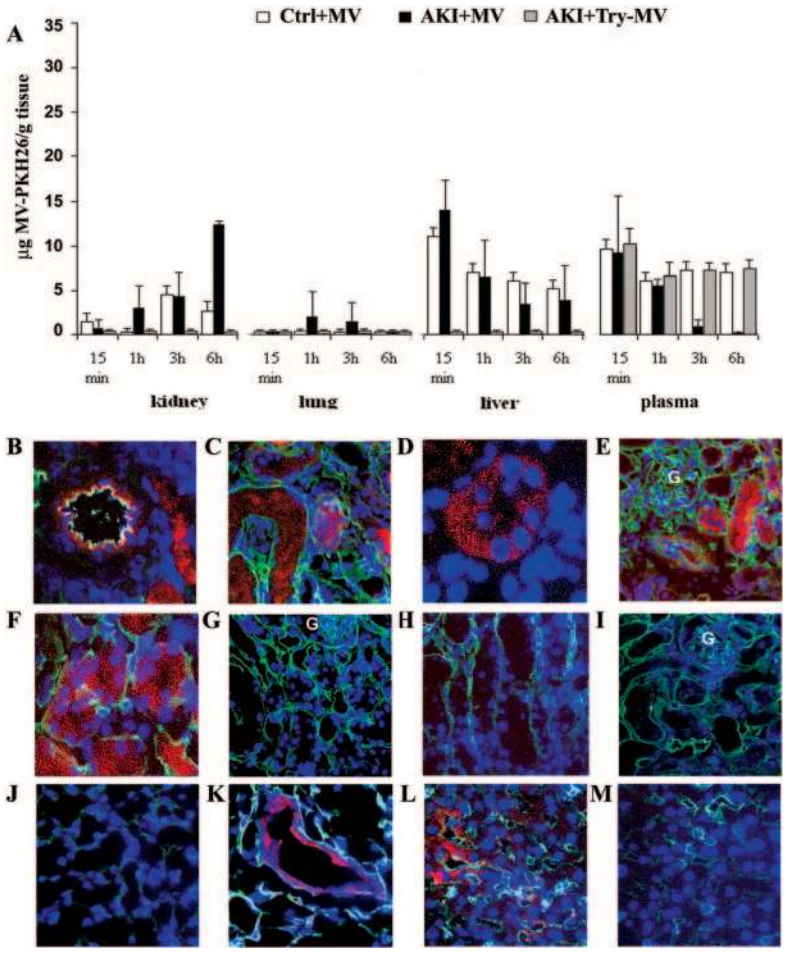

Figure 10. Distribution of microvesicles (MVs) after *in vivo* injection. (A) Quantification by spectrofluorimetric analyses of the amount of PKH26-labeled MVs, treated or not with trypsin, in different organs of acute kidney injury (AKI) and healthy mice (control+MV) as described in Concise Methods. The amount of MV-PKH26 is expressed in μg/g of dry tissue or μg/μl of plasma. (B–M): Representative confocal micrographs of frozen tissue sections of mice injected with PKH26-labeled MVs (red) and stained with vWF (B and K) or laminin (C–J, L, M) antibodies (green staining). MVs were detectable, after 1 h, within the endothelial cells of a renal vessel stained with anti-vWF antibody and within the lumen of injured tubules (B); after 3 h several tubular cells contained red MVs (C, D); at 6 h (E, F) the number of tubular cells containing red MVs was enhanced. MVs treated with trypsin were not detected in the kidney (G). In a normal control mouse, red MVs were not detected in tubular cells (H). In the lung, red MVs were not detected in the alveolar capillaries (J), whereas they were located in the endothelial cells of a large vessel (K). Liver accumulation of red MVs was detected both in normal controls (not shown) and in AKI mice (L). No signal was observed in specimens of AKI not injected with labeled MVs (I = kidney; M = liver). Nuclei were counterstained with Hoechst dye. B, C, E, G-M, original magnifications: ×400; D and F, original magnifications: ×630. G, glomeruli. Per each group (control+MV, AKI+MV, AKI+trypsin treated MV) and each time points three animals were studied with similar results.

grin, α5-integrin, α6-integrin (BioLegend, San Diego, CAUSA). FITC or PE mouse nonimmune isotypic IgG (Dako Cytomation) were used as control.

By cytofluorimetric analyses MVs, from human fibroblasts, were detected mainly below the forward scatter signal corresponding to 1-μm beads (not shown); when determined by Zetasizer, the size of MVs was 180 nm (mean value). Cytofluorimetric analyses showed that MVs form human fibroblasts did not express adhesion molecules expressed on MVs derived from MSCs (CD44, CD29, CD73, ICAM-1, α4-integrin, αvβ3-integrin, α5-integrin, α6-integrin; not shown).

In vitro Isolation and Expansion of TECs

Kidneys were obtained from healthy female C57 mice. Kidneys were finely minced with scissors and then were forced through a 40-μm pore filter (Becton Dickinson, San Jose, CA); the glomerular part and aggregated remained on the surface of filter while tubular cells were collected. After 2 washings in PBS (Lonza), the cell suspension was plated in a T25 flask (Becton Dickinson) in the presence of DMEM (Sigma) and 10% FCS. We changed media after 5 d to eliminate nonliving cells. TECs were characterized for their positive staining of cytokeratin, actin, alkaline phosphatase, aminopeptidase A, and megalin, and for negative staining for von Willebrand factor, CD45, nephrin, and desmin.

Incorporation of MVs in TECs

To study the capacity of MVs to incorporate into TECs, we incubated 50 μg/ml of MVs, labeled with PKH-26 dye, for 30 min at 37 °C. We studied the incorporation by FACS analyses and confocal microscopy.

To investigate the role of adhesion molecules expressed by MV surface in the incorporation in target cells, we preincubated MVs (15 min at 4 °C) with blocking antibodies (1 μg/ml) against the identified adhesion molecules anti-α4-integrin (Biolegend), α5-integrin (Biolegend), CD29 (β1-integrin) (Becton Dickinson), CD44 (Becton Dickinson) or with sHA (100 μg/ml from Rooster comb; Sigma) before the incubation with the cells.

Immunofluorescence for Human Protein Expression in TECs

Indirect immunofluorescence was performed on TECs cultured on chamber slides (Nalgen Nunc International, Rochester, NY) and stimulated for 1 and 2 d in the presence of 30 μg of different preparations of MVs. The cells were fixed in 4% paraformaldehyde containing 2% sucrose and permeabilized with HEPES-Triton X100 buffer (Sigma). The following antibodies were used: rabbit anti-human POLR2E (Abcam, Cambridge Science Park, UK) and rabbit anti-human Sumo-1 (AbCam). Omission of the primary antibodies and substitution with nonimmune rabbit IgG were used as controls. Alexa

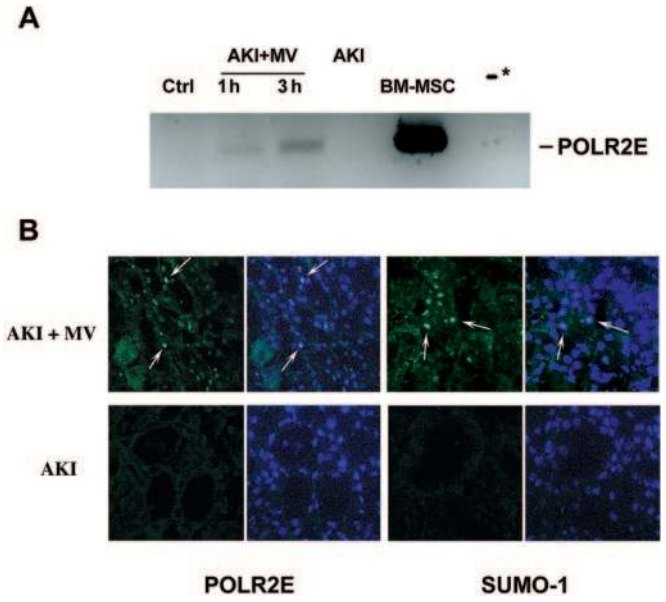

Figure 11. Detection of human mRNA and human protein expression in kidneys of mice treated with human mesenchymal stem cell (MSC)-derived microvesicles (MVs). (A) Representative RT-PCR of acute kidney injury (AKI) mice untreated (AKI) or treated with 15 μg of MSC-derived MVs (AKI+MV) and sacrificed 1 and 3 h after MV injection. Bands of PCR products specific for human POLR2E of the expected size (90 bp) were detected in a 4% agarose gel electrophoresis in AKI treated with MVs but not in untreated AKI or in normal murine kidney (Ctrl). As positive control the extract of human bone marrow-derived MSCs (BM-MSC) was used. The asterisk indicates the control without cDNA. (B) Representative confocal micrographs showing the nuclear expression of human POLR2E and SUMO-1 proteins in kidney sections of AKI mice treated or not with MVs and sacrificed 48 h later. Nuclei were counterstained with Hoechst dye. Original magnification: ×400. Arrows indicate positive nuclei. The right panels of each show merge for the SUMO-1 or POLR2E staining and the nuclear staining with Hoechst. Eight animals per groups were examined with similar results.

Fluor 488 anti-rabbit (Molecular Probes) was used as secondary antibody. Confocal microscopy analysis was performed using a Zeiss LSM 5 Pascal Model Confocal Microscope (Carl Zeiss International, Germany). Hoechst 33258 dye (Sigma) was added for nuclear staining.

Cell Proliferation, Apoptosis Assays, and Release of HGF and MSP

TECs were seeded at 4000 cells/well into 96-well plates in DMEM (Sigma) deprived of FCS. DNA synthesis was detected as incorporation of BrdU into the cellular DNA after 48 h of culture. Cells were then fixed with 0.5 M ethanol/HCl and incubated with nuclease to digest the DNA. BrdU incorporated into the DNA was detected using an anti-BrdU peroxidase-conjugated antibody and visualized with a soluble chromogenic substrate (Roche Applied Science, Mannheim, Germany). Optical density was measured with an ELISA reader at 405 nm. Apoptosis was evaluated using the TUNEL assay (ApopTag Oncor, Gaithersburg, MD) as described previously.[38] As apoptotic stimuli, we used serum deprivation or stimulation with 100 ng/ml of vincristine (Sigma) and 5 μg/ml of *cis*-platinum (Sigma) in DMEM plus 3% FCS.

To evaluate the production of HGF and MSP, 1×10^5 TECs were cultured with or without MV (30 μg/ml) and, after 24 and 48 h of incubation, the supernatants were recovered and MSP-1and HGF production measured by ELISA (Raybiotech, Norcross GA) in accordance with manufacturer's instruction.

Gene Array Analysis

RNA extraction, Samples Labeling and Hybridization on BeadChips

RNA was extracted from MVs using TRIZOL reagent (Invitrogen) following the procedure suggested by the manufacturer. Total RNA was quantified spectrophotometrically (Nanodrop ND-1000, Wilmington DE). cRNA was synthesized using three different quantities of total RNA (0.25 μg, 0.5 μg, and 1 μg). cRNA synthesis and labeling was done using Illumina RNA Amplification Kit (Ambion) following the procedure suggested by manufacturer. Sentrix Human-6 Expression BeadChip hybridization, washing, and staining were also done as suggested by the manufacturer. Arrays were scanned on Illumina BeadStation 500 (Illumina, San Diego, CA). Transcripts present in the MVs were defined as those characterized by a positive linear relation between the transcript signal detected by the microarray analysis and the amount of total RNA hybridized.[18]

Microarray Data Analysis

The analysis was done hybridizing arrays with labeled-cRNA produced using three different concentrations of total RNA extracted from two independent preparations of MVs. BeadChip array data quality control was performed using Illumina BeadStudio software, version 1.3.1.5. Transcript average intensity signals were calculated with BeadStudio without background correction. Raw data were analyzed using Bioconductor.[39] Average transcript intensities were $\log_2$ transformed and normalized by the Loess method.[20]

A simple statistical linear model[18] was used to identify transcript signals linearly correlated to the increment of total RNA concentration used to prepare cRNA. In equation (1), y_{ij} is the observed expression level for transcript i in sample j (j = 1,. . . ,6), μ is the average expression level of transcript I, and β_{RNA} represents the effect of total RNA concentration on the expression level of transcript i. ε represents random error for transcript i and sample j, and it is assumed to be independent for each transcript and sample, and normally distributed with mean 0 and variance σ^2.

$$y_{ij} = m_i + b_{RNA} + e_{ij} \quad (1)$$

Transcripts characterized by a model with $P \leq 0.05$, $r^2 \geq 0.8$, and a positive slope were selected (239).

Transcripts annotation and data mining were performed using IPA 4.0 software (www.ingenuity.com). Microarray data were deposited on GEO database (http://www.ncbi.nlm.nih.gov/projects/geo/) as geo accession GSE12243.

Quantitative Real Time PCR

Quantitative real time PCR was performed as described previously.[40] Quantitative real-time PCR was performed on total RNA extracted from cells used to produce MVs and from an MV preparation different from those used for microarray analysis. Cell cDNA was used to evaluate primers efficiency. The primers used for real time PCR are shown in Table 4. First-strand cDNA was produced from total RNA using the High Capacity cDNA Reverse Transcription Kit (Applied Biosystems, Foster City, CA). Briefly, 200 to 400 ng mRNA, 2 μl RT buffer, 0.8 μl dNTP mixture, 2 μl RT random primers, 1 μl MultiScribe reverse transcriptase, and 4.2 μl nuclease-free water were used for each cDNA synthesis. After the reverse transcription, cDNA was stored at −20 °C. Twenty microliters of RT-PCR mix, containing 1X SYBR GREEN PCR Master Mix (Applied Biosystems), 100 nM of each primer, and 0 μl, 1 μl, and 2 μl of MV cDNA, were assembled using a 48-well StepOne Real Time System (Applied Biosystems). Negative cDNA controls (no cDNA) were cycled in parallel with each run.

Reverse Transcriptase PCR (RT-PCR)

Total RNA extracted from TECs or from kidneys of SCID mice was submitted to RT-PCR[41] using the primer for human *POLR2E* and *SUMO-1* reported in Table 4. Bands of the expected size (90 bp) were detected in a 4% agarose gel after electrophoresis. cDNA from a preparation of human bone marrow MSC was used as positive control.

SCID Mice Model of AKI

Studies were approved and conducted in accordance with the National Institute of Health Guide for the Care and Use of Laboratory Animals. As described previously,[5,6,30] a model of rhabdomyolisis-induced AKI was performed in male SCID mice (7 to 8 wk old) (Charles River Laboratories), by intramuscular injection with hypertonic glycerol (8 ml/kg body weight of 50% glycerol solution) into the inferior hind limbs (Figure 6). Intramuscular injection of glycerol induces myolisis and hemolysis causing toxic and ischemic tubular injury.[5,6] On day 3 after glycerol administration, mice received an intravenous injection into the tail vein of 15 μg of MVs from MSCs treated with sHA, or trypsin or RNase-MVs, or 15 μg of MVs from human fibroblasts, or 75,000 BM-MSCs in 150 μl saline, or saline alone. The following groups were studied: group 1, AKI group; group 2, AKI plus 15 μg MVs injected 3 d after induction of renal injury; group 3, AKI plus 15 μg RNase-treated MVs; group 4, AKI plus 75,000 human MSCs; group 5, AKI plus 15 μg of MVs from fibroblasts; group 6, AKI plus 15 μg MVs from MSCs treated with sHA; group 7, AKI plus 15 μg MVs from MSCs treated with trypsin. The amount of 15 μg MVs was chosen because it corresponds to the amount released overnight by 75,000 MSCs. For *in vivo* detection of proliferation, mice were administrated an injection of BrdU (100 mg/kg) intraperitoneally for 2 successive days before being killed. In each group, mice were killed at different time intervals (day 3 [n = 10], day 4 [n = 8 per group], day 5 [n = 8 per group], day 8 [n = 8 per group] and day 15 [n = 6 per group] after glycerol administration) and kidneys and samples for BUN and creatinine determination were collected.

Kidney tissues were processed for histology, immunohistochemistry, immunofluorescence and transmission electron microscopy.

Morphologic Studies

For renal histology 5-μm-thick paraffin kidney sections were routinely stained with hematoxylin and eosin (Merck, Darmstadt, Germany). Luminal hyaline casts and cell lose (denudation of tubular basement membrane) were assessed in nonoverlapping fields (up to 28 for each section) using a 40x objective (high power filed, HPF). Number of casts and tubular profiles showing necrosis were recorded in a single-blind fashion.[4]

Transmission electron microscopy was performed on Karnovsky's-fixed, osmium tetraoxide-postfixed tissues and embedded in epoxy resin according to standard procedures.[42] Ultrathin sections were stained with uranyl acetate and lead citrate and were examined with a Jeol JEM 1010 electron microscope. Transmission electron microscopy was also performed on MVs or on cultured MSCs releasing MVs processed as described above. For scanning electron microscopy MVs were fixed in Karnovsky fixative, dehydrated in alcohol, dried on glass surface and coated with gold by sputter coating. The specimens were examined in a scanning Jeol T300 electron microscope. Images were obtained via secondary electron at a working distance of 15 to 25 mm and an accelerating voltage of 20 to 25 kV.

Immunohistochemistry for detection of proliferation of tubular cells was performed as described previously.[9] Kidney sections were subjected to antigen retrieval, and slides were blocked and labeled with 1:25 dilution of monoclonal anti BrdU antibody (Dako Cytomation) or 1:400 of monoclonal anti-PCNA (Santa Cruz Biotechnology, Santa Cruz CA). Immunoperoxidase staining was performed using 1:300 dilution of anti-mouse HRP (Pierce, Rockford IL). Scoring for BrdU- and PCNA -positive cells was carried out by counting the number of positive nuclei per field in 10 randomly chosen sections of kidney cortex using 40x magnification. Confocal microscopy analysis was performed on frozen sections for localization of PKH26-labeled MVs in different murine organs and for detection of specific human proteins POLR2E and SUMO-1. Section were blocked and labeled with rabbit anti-human POLR2E (Abcam) (1:300 dilution) or rabbit anti-human Sumo-1 (Abcam) (1:300 dilution) or rabbit anti Laminin (Sigma) (1:100 dilution) or rabbit anti von Willebrand factor (Dako Cytomation) (1:100 dilution). Omission of the primary antibodies or substitution with nonimmune rabbit IgG were used as controls. Alexa Fluor 488 anti-rabbit (Molecular Probes) was used as secondary antibody.

Table 4. Human primers for real-time quantitative PCR

	Forward	Reverse
POLR2E	5′-GCTCTGGAAAATCCGCAAGA-3′	5′-TCCTCCAGGGTCTGGTCAAG-3′
SENP2/SUMO1	5′-AAATAAGATCGACCAATGCAAGTG-3′	5′-TCACAGTCCAGGAGTGAAGTAATCA-3′
RBL1	5′-GAGAACTGGGTCCTTAGCACTATTTT-3′	5′-ACACGTCCATATCTTCCTTCGTAAC-3′
CXCR7	5′-TGGGTTACAAAGCTGCCATCTA-3′	5′-TGGCTGTGCTGTGCGCT-3′
LTA4H	5′-CCTATCGCTTTGAGCAAAAATCA-3′	5′-GTGTTCCTTCCCAGAAGTCTGTTC-3′

Plasma BUN and Creatinine

Blood samples for measurement of BUN and plasma creatinine were collected before and 3, 4, 5, 8 and 15 d after glycerol-induced AKI. Creatinine concentrations were determined using a Beckman Creatinine Analyzer II (Beckman Instruments, Inc., Fullerton, CA).[6] Creatinine levels that exceeded 0.3 mg/dl were considered abnormal (normal range in our laboratory: 0.1 to 0.3 mg/dl). BUN was assessed in heparinized blood using a Beckman Synchrotron CX9 automated chemistry analyzer (Beckman).

Spectrofluorimetric Detection of MVs in Different Tissues after *In Vivo* Injection

To evaluate the amount of MVs in different murine organs, we injected intravenously AKI or healthy mice with 100 μg of PKH-26 labeled MVs treated or not with trypsin. Mice were sacrificed after 15 min, 1, 3, and 6 h and liver, lungs, kidneys, and blood were recovered. The content of PKH-26 in different samples was measured after lipid extraction with chloroform-isopropyl alcohol (1:1 vol/vol) and 0.125% SDS (Sigma) of homogenized tissues (Tissue Ruptor, Quiagen) or plasma. The fluorescence intensity of PKH-26-containing lipid extracts were measured with Fluoromax-4 spectrofluorimeter (Horiba Jobin Yvon_Edison NJ). Excitation wavelength was positioned at 550 nm; emission wavelength was set at 567 nm. Calibration values for maximum and minimum were obtained using 20 μg/ml and decreasing concentration until 1 μg/ml of lipid extracts of PKH26-labeled MV. Each lipid sample (from different organs and plasma) was analyzed in PBS (Sigma) containing 0.1% triton X100 (Sigma). As negative control, we measured fluorescence intensity in lipids extracted from untreated mice. Data were expressed as micrograms per gram of dry tissue or micrograms per microliter plasma.

Statistical Analysis

Statistical analysis was performed by using the *t* test, ANOVA with Newmann-Keuls, or ANOVA with Dunnet's multicomparison tests, as appropriate. A p value of <0.05 was considered significant.

ACKNOWLEDGMENTS

This work was supported by Italian Ministry of University and Research COFIN and ex60%, by Regione Piemonte, by Progetto Alfieri CRT, by the Italian Ministry of Health, by Progetto S. Paolo and by Fresenius Medical Care.

DISCLOSURES

M. C. D. and G. C. are named inventors on related patent applications.

REFERENCES

1. Phinney DG, Prockop DJ: Concise review: Mesenchymal stem/multipotent stromal cells: The state of transdifferentiation and modes of tissue repair–Current views. *Stem Cells* 25: 2896–2902, 2007
2. Humphreys BD, Bonventre JV: Mesenchymal stem cells in acute kidney injury. *Annu Rev Med* 59: 311–325, 2008
3. Morigi M, Imberti B, Zoja C, Corna D, Tomasoni S, Abbate M, Rottoli D, Angioletti S, Benigni A, Perico N, Alison M, Remuzzi G: Mesenchymal stem cells are renotropic, helping to repair the kidney and improve function in acute renal failure. *J Am Soc Nephrol* 15: 1794–1804, 2004
4. Morigi M, Introna M, Imberti B, Corna D, Abbate M, Rota C, Rottoli D, Benigni A, Perico N, Zoja C, Rambaldi A, Remuzzi A, Remuzzi G: Human bone marrow-mesenchymal stem cells accelerate recovery of acute renal injury and prolong survival in mice. *Stem Cells* 26: 2075–2082, 2008
5. Herrera MB, Bussolati B, Bruno S, Fonsato V, Romanazzi GM, Camussi G: Mesenchymal stem cells contribute to the renal repair of acute tubular epithelial injury. *Int J Mol Med* 14: 1035–1041, 2004
6. Herrera MB, Bussolati B, Bruno S, Morando L, Mauriello-Romanazzi G, Sanavio F, Stamenkovic I, Biancone L, Camussi G: Exogenous mesenchymal stem cells localize to the kidney by means of CD44 following acute tubular injury. *Kidney Int* 72: 430–441, 2007
7. Togel F, Hu Z, Weiss K, Isaac J, Lange C, Westenfelder C: Administered mesenchymal stem cells protect against ischemic acute renal failure through differentiation-independent mechanisms. *Am J Physiol Renal Physiol* 289: 31–42, 2005
8. Lange C, Togel F, Ittrich H Clayton F, Nolte-Ernsting C, Zander AR, Westenfelder C: Administered mesenchymal stem cells enhance recovery from ischemia/reperfusion-induced acute renal failure in rates. *Kidney Int* 68: 1613–1617, 2005
9. Bi B, Schmitt R, Israilova M, Nishio H, Cantley LG: Stromal cells protect against acute tubular injury via an endocrine effect. *J Am Soc Nephrol* 18: 2486–2496, 2007
10. Fang TC, Alison MR, Cook HT, Jeffery R, Wright NA, Poulsom R: Proliferation of bone marrow-derived cells contributes to regeneration after folic acid-induced acute tubular injury. *J Am Soc Nephrol* 16: 1723–1732, 2005
11. Broekema M, Harmsen MC, Koerts JA, Petersen AH, van Luyn MJ, Navis J, Popa ER: Determinants of tubular bone marrow-derived cell engraftment after renal ischemia/reperfusion in rats. *Kidney Int* 68: 2572–2581, 2005
12. Tögel F, Yang Y, Zhang P, Hu Z, Westenfelder C: Bioluminescence imaging to monitor the in vivo distribution of administered mesenchymal stem cells in acute kidney injury. *Am J Physiol Renal Physiol* 295: F315–F321, 2008
13. Duffield JS, Park KM, Hsiao LL, Kelley VR, Scadden DT, Ichimura T, Bonventre JV: Restoration of tubular epithelial cells during repair of the postischemic kidney occurs independently of bone marrow-derived stem cells. *J Clin Invest* 115: 743–755, 2005
14. Humphreys BD, Valerius MT, Kobayashi A, Mugford JW, Soeung S, Duffield JS, McMahon AP, Bonventre JV: Intrinsic epithelial cells repair the kidney after injury. *Cell Stem Cell* 2: 284–291, 2008
15. Schorey JS, Bhatnagar S: Exosome function: From tumor immunology to pathogen biology. *Traffic* 9: 871–881, 2008
16. Morel O, Toti F, Hugel B, Freyssinet JM: Cellular microparticles: A disseminated storage pool of bioactive vascular effectors. *Curr Opin Hematol* 11: 156–164, 2004
17. Ratajczak J, Miekus K, Kucia M Zhang J, Reca R, Dvorak P, Ratajczak MZ: Embryonic stem cells-derived microvesicles reprogram hematopoietic progenitors: Evidence for horizontal transfer of mRNA and protein delivery. *Leukemia* 20: 847–856, 2006
18. Deregibus MC, Cantaluppi V, Calogero R, Lo Iacono M, Tetta C, Biancone L, Bruno S, Bussolati B, Camussi G: Endothelial progenitor cell-derived microvescicles activate an angiogenic program in endothelial cells by a horizontal transfer of mRNA. *Blood* 110: 2440–2448, 2007
19. Valadi H, Ekström K, Bossios A, Sjöstrand M, Lee JJ, Lötvall JO: Exosome-mediated transfer of mRNAs and microRNAs is a novel mechanism of genetic exchange between cells. *Nat Cell Biol* 9: 654–659, 2007

20. Bolstad BM, Irizarry RA, Astrand M, Speed TP: A comparison of normalization methods for high density oligonucleotide array data based on variance and bias. *Bioinformatics* 19: 185–193, 2003
21. Cantley LG: Adult stem cells in the repair of the injured renal tubule. *Nat Clin Prac Nephrol* 1: 22–32, 2005
22. Tögel F, Weiss K, Yang Y, Hu Z, Zhang P, Westenfelder C: Vasculotropic, paracrine actions of infused mesenchymal stem cells are important to the recovery from acute kidney injury. *Am J Physiol Renal Physiol* 292: 1626–1635, 2007
23. Imberti B, Morigi M, Tomasoni S, Rota C, Corna D, Longaretti L, Rottoli D, Valsecchi F, Benigni A, Wang J, Abbate M, Zoja C, Remuzzi G: Insulin-like growth factor-1 sustains stem cell mediated renal repair. *J Am Soc Nephrol* 18: 2921–2928, 2007
24. Weyrich AS, Kraiss LW, Zimmerman GA: Trading places: mRNA transfer between cells. *Blood* 110: 2219, 2007
25. Janowska-Wieczorek A, Majka M, Kijowski J, Baj-Krzyworzeka M, Reca R, Turner AR, Ratajczak J, Emerson SG, Kowalska MA, Ratajczak MZ: Platelet-derived microparticles bind to hematopoietic progenitor cells and enhance their engraftment. *Blood* 98: 3143–3149, 2001
26. Baj-Krzyworzeka M, Majka M, Pratico D, Ratajczak J, Vilaire G, Kijowski J, Reca R, Janowska-Wieczorek A, Ratajczak MZ: Platelet-derived microparticles stimulate proliferation, survival, adhesion, and chemotaxis of hematopoietic cells. *Exp Hematol* 30: 450–459, 2002
27. Taraboletti G, D'Ascenzo S, Borsotti P, Gavazzi R, Pavan A, Dolo V: Shedding of the matrix metalloproteinases MMP-2, MMP-9 and MT1-MMP as membrane vesicle-associated components by endothelial cells. *Am J Pathol* 160: 673–680, 2002
28. Acker J, Wintzerith M, Vigneron M, Kédinger C: Primary structure of the second largest subunit of human RNA polymerase II (or B). *J Mol Biol* 226: 1295–1299, 1992
29. Cantaluppi V, Biancone L, Romanazzi GM, Figliolini F, Beltramo S, Galimi F, Camboni MG, Deriu E, Conaldi P, Bottelli A, Orlandi V, Herrera MB, Pacitti A, Segoloni GP, Camussi G: Macrophage stimulating protein may promote tubular regeneration after acute injury. *J Am Soc Nephrol* 19: 1904–1918, 2008
30. Karihaloo A, Nickel C, Cantley LG: Signals which build a tubule. *Nephron Exp Nephro* 100: e40–e45, 2005
31. Matsumoto K, Nakamura T. Hepatocyte growth factor: Renotropic role and potential therapeutics for renal diseases. *Kidney Int* 59:2023–2038, 2001
32. Kunter U, Rong S, Boor P, Eitner F, Müller-Newen G, Djuric Z, van Roeyen CR, Konieczny A, Ostendorf T, Villa L, Milovanceva-Popovska M, Kerjaschki D, Floege J: Mesenchymal stem cells prevent progressive experimental renal failure but maldifferentiate into glomerular adipocytes. *J Am Soc Nephrol* 18: 1754–1764, 2007
33. Bussolati B, Bruno S, Grange C, Buttiglieri S, Deregibus MC, Cantino D, Camussi G: Isolation of renal progenitor cells from adult human kidney. *Am J Pathol* 166: 545–555, 2005
34. Pittenger MF, Mackay AM, Beck SC, Jaiswal RK, Douglas R, Mosca JD, Moorman MA, Simonetti DW, Craig S, Marshak DR: Multilineage potential of adult human mesenchymal stem cells. *Science* 284: 143–147, 1999
35. Granot D, Kunz-Schughart LA, Neeman M: Labeling fibroblasts with biotin-BSA-GdDTPA-FAM for tracking of tumor-associated stroma by fluorescence and MR imaging. *Magn Reson Med* 54: 789–797, 2005
36. Mesri M, Altieri DC: Leukocyte microparticles stimulate endothelial cell cytokine release and tissue factor induction in JNK1 signaling pathway. *J Biol Chem* 274: 23111–23118, 1999
37. Baj-Krzyworzeka M, Szatanek R, Weglarczyk K, Baran J, Urbanowicz B, Brański P, Ratajczak MZ, Zembala M: Tumour-derived microvesicles carry several surface determinants and mRNA of tumour cells and transfer some of these determinants to monocytes. *Cancer Immunol Immunother* 55: 808–8018, 2006
38. Bussolati B, Deambrosis I, Russo S, Deregibus MC, Camussi G: Altered angiogenesis and survival in human tumor-derived endothelial cells. *FASEB J* 17: 1159–1161, 2003
39. Gentleman RC, Carey VJ, Bates DM, Bolstad B, Dettling M, Dudoit S, Ellis B, Gautier L, Ge Y, Gentry J, Hornik K, Hothorn T, Huber W, Iacus S, Irizarry R, Leisch F, Li C, Maechler M, Rossini AJ, Sawitzki G, Smith C, Smyth G, Tierney L, Yang JY, Zhang J: Bioconductor: Open software development for computational biology and bioinformatics. *Genome Biol* 5: R80, 2004
40. Collino F, Bussolati B, Gerbaudo E, Marozio L, Pelissetto S, Benedetto C, Camussi G: Preeclamptic sera induce nephrin shedding from podocytes through endothelin-1 release by endothelial glomerular cells. *Am J Physiol Renal Physiol* 294: F1185–1194, 2008
41. Fonsato V, Buttiglieri S, Deregibus MC, Bussolati B, Caselli E, Di Luca D, Camussi G: PAX2 expression by HHV-8-infected endothelial cells induced a proangiogenic and proinvasive phenotype. *Blood* 111: 2806–2815, 2008
42. Camussi G, Kerjaschki D, Gonda M, Nevins T, Rielle JC, Brentjens J, Andres G: Expression and modulation of surface antigens in cultured rat glomerular visceral epithelial cells. *J Histochem Cytochem* 37: 1675–1687, 1989

See related editorial, "Microvesicles from Mesenchymal Stromal Cells Protect against Acute Kidney Injury," on pages 927–928.